Hydrogen Transfer in the Formation and Destruction of Retrograde Products in Coal Conversion[†]

Donald F. McMillen and Ripudaman Malhotra*

SRI International, 333 Ravenswood Avenue, Menlo Park, California 94025

Received: October 31, 2005; In Final Form: December 16, 2005

The conversion of coals to volatiles or liquids during pyrolysis and liquefaction is notoriously limited by the formation of retrograde products. Analysis of literature data for coals with grafted structures and for polymeric coal models demonstrates that the formation of volatile products from these materials does not correlate primarily with the weakness of the original bonding but correlates with the facility for retrogressive reaction. This analysis suggests further that simple recombination of resonance-stabilized radicals does not tend to yield true retrograde products, except in the case of aryloxy radicals. For pure hydrocarbon structural elements, radical addition to aromatic systems appears to be a key class of retrograde reactions, where the key factor is the kinetics of radical or H-atom loss from a cyclohexadienyl intermediate. We have used a mechanistic numerical model with a detailed set of radical reactions and thermochemically based kinetic parameters operating on a limited set of hydrocarbon structures to delineate important factors in mitigating retrograde processes. The modeling results show (1) how the "better" radical scavengers may reduce retrograde reaction at short reaction times but actually tend to increase it at longer times; (2) that the beneficial effects of H_2 pressure at short reaction times are *not* primarily due to lowering of harmful radical concentrations by scavenging, *nor* to the maintenance of donor content; (3) that the benefit is due to the small population of free H-atoms thus produced, which are very active in causing increased scission of strong bonds; and (4) that under some conditions retrograde products are actually generated *faster* with added H_2, but at longer reaction times and higher temperatures this temporary disadvantage of H_2 is overcome by increased hydrogenolysis of those earlier-produced retrograde products. Thus, not only the cleavage of critical bonds in the original coal structures but also the *net* prevention of retrogression may be due to the H-transfer-induced cleavage of strong bonds.
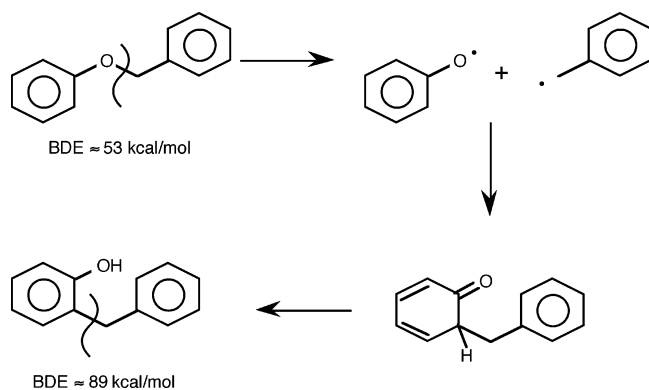
Introduction

Research and development on the upgrading of fossil resources has languished following the global collapse of oil prices in 1986 and again in 1998. Recent increases in the price of crude oil, together with mounting global warming concerns, have returned energy supply and conversion questions to the center of the national consciousness.[1,2] The resource limitations and inflamed foreign relations will doubtless increase calls for "fundamentally new scientific approaches to coal utilization", a "complete switch to renewable resources", or simply for all-out efforts to drastically increase the extraction of remaining fossil resources.[3] The desire for "fundamentally new approaches" is welcome but needs to be guided by−rather than divorced from−the thermodynamic, kinetic, and chemical engineering realities that have ineluctably governed the fossil-fuel technology painstakingly developed over the last 75 years.

The mechanistic picture of the thermal conversion of coals to liquid and gaseous products that held sway for 50 years was spontaneous thermal scission, or homolysis, of inherently weak bonds followed by scavenging of those radicals by H-donor structures. In previous work, we and others have shown that this picture is incomplete and must be augmented by induced cleavage of strong bonds.[4−9] In this pathway, the transfer of hydrogen atoms or carbon-centered radicals induces the scission of bonds that otherwise would not break at coal liquefaction temperatures. Such pathways for induced bond cleavage were

well recognized in the technology of thermal, high-temperature hydrocracking but were not expected at around 650 K, where coal liquefaction and pyrolysis are observed to begin.[10] These temperatures are well below those where free H-atoms are known to approach thermal equilibrium with H_2.

Our focus in this paper is on retrogressive reactions (i.e., the formation of strong bonds between coal structures to yield more refractory products) in nonpolar systems, either pure hydrocarbons or structures with ether linkages. Phenols, carboxylic acids, and other oxygen compounds can and do form retrograde products by coupling reactions, and these can be very important. Indeed, a typical bituminous coal contains roughly 1 oxygen for every 10 carbons and 1 phenolic OH for every 20 carbon atoms. Phenolic structures provide a strong thermodynamic driving force for the elimination of water as well as a general tendency to promote reaction via polar intermediates,[11] but condensation reactions are nevertheless kinetically hindered for simple phenols. We have recently delineated several cases of rapid coupling of phenolic structures that involve both condensation and de-hydro coupling.[12] Scheme 1 illustrates one simple example of the latter reaction type in which coupling of resonance-stabilized radicals actually leads to a moderately stable retrograde product. As we saw evident[13] through rate measurements of the microscopic reverse process, namely, the cleavage via tautomerization of benzyl phenols, hydrogen can be lost as a proton from a weakly bound keto intermediate whose polar carbonyl group stabilizes the resulting anion, leading to facile rearrangement.

6758 *J. Phys. Chem. A, Vol. 110, No. 21, 2006*

McMillen and Malhotra

SCHEME 1: Recombination of a Phenoxy Radical through Carbon with a Benzyl Radical Leading to Benzylphenol

BDE ≈ 53 kcal/mol

BDE ≈ 89 kcal/mol

TABLE 1: Label Recovery from Pyrolysis of Grafted Coal Structures

grafted coal structure	BDE (kcal/mol)	$t_{1/2}$ (650 °C)	% label recovered in volatiles[a]
coalO$-n$-C$_3$H$_7$	62	300 ms	39
coalO$-$CH$_2$Ph	53	<2 ms	9

[a] Pyrolysis in a temperature-ramped grid at rates of about 1000 k/s to a maximum temperature of 800 °C (from ref 17).
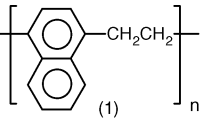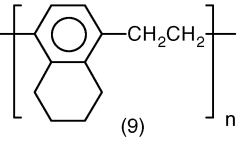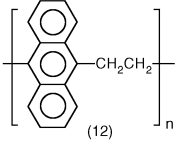
According to the conventional view of coal liquefaction and pyrolysis, retrogressive reactions in nonpolar systems result primarily from recombination of radical species. In this paper, we show the importance of radical additions and H-transfers in retrogressive reactions in these systems. We begin by reexamining some published results that demonstrate a disconnect between the weakness of bonds and char yields that was not necessarily highlighted by their original authors. These literature data, published in an era when energy research was being actively pursued, include "hybrid" conversion experiments using mixtures of real coals and model coal structures and also the pyrolysis of polymeric coal models. These studies were chosen because they clearly reflect, as well as give insight into, the formation of strong C$-$C or C$-$O bonds, the so-called retrograde reactions.

To study the thermochemical factors influencing these retrograde reactions, we made use of a mechanistic numerical model, similar to one we used earlier to probe the chemistry of induced bond scission.[14] Just as strong bonds can only be broken$-$in the free-radical realm$-$via a β-scission that follows transfer of H$^\bullet$ or R$^\bullet$, strong bonds cannot be formed to yield a permanent retrograde product without H$^\bullet$ or R$^\bullet$ transfer to lock an initially formed adduct into place. It is not surprising that the model shows hydrogen donors to be helpful in preventing retrogression; that fact has been known empirically for more than 50 years. More interesting are the ways in which the donor is helpful$-$ways that were not readily intuited, notwithstanding the apparent simplicity of the model itself.

Analysis of Literature Data

Pyrolysis of Grafted Coals. In a noteworthy effort to eliminate some of the uncertainties encountered on one hand in studies of "real" coals and on the other hand in studies of model compounds, Zabransky and Stock covalently grafted isotopically labeled groups to real coals through their phenolic $-$OH groups and then subjected the grafted coals to pyrolysis using a resistively heated wire grid reactor. Deuterium- and ^{13}C-labeling of various hydrogens and carbons in the grafted groups, followed by mass spectrometric analysis of the gaseous products, enabled identifiable portions of the grafted structures to be tracked with a degree of certitude that is not possible with real coals.[15$-$17] As the authors point out, the results showed that indeed the cleavage of strong bonds by β-scission, after either H-abstraction from an alkyl group or H-transfer to an aromatic group, provides important routes for fragmentation of the grafted structures. The focus of these papers was on the pathways by which the coal structures fall apart, but the results also indicate
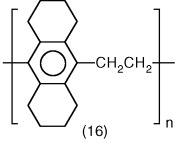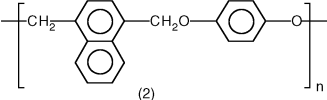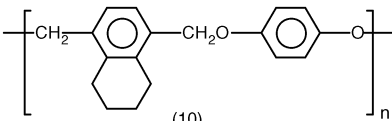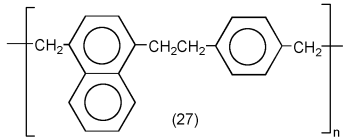
that the impact of retrogressive reactions on devolatilization of even small pendant groups is quite profound, and give some hints about the character of the retrograde processes.

As the data[17] in Table 1 show, the volatiles from O-alkylated* coals contain a substantially larger fraction of isotopic label as compared with those from O-benzylated* coals: the volatiles from O-benzylated* coal contained only 9% of the original label, one-fourth of that found in the O-alkylated* coal, although the bond strength for the O-benzyl graft is some 10 kcal/mol weaker than the O-alkyl graft. Since the higher volatiles yield in the case of the O-nPr coal is not due to faster cleavage (at least via homolysis), it must be due to slower retrogression. By comparing the alkene/alkane ratios in the products of various grafted coals, Zabransky and Stock argued persuasively that the C$_3$ hydrocarbon from the O-nPr coal comes primarily from alkyl radical fragments produced via homolysis,[18] rather than through β-scission in a Rice$-$Herzfeld alkane pyrolysis sequence, which would offer an alternative to homolysis for scission of the aliphatic graft. The successful homolysis of aliphatic linkages that are significantly stronger than the weak bond in the O-benzyl coal thus fixes the cause for the low yields of toluene on the proclivity of aromatic structures for undergoing retrograde reactions.

Two likely explanations for more facile retrograde reactions with the O-benzyl coal seem to be either that a homolytically generated benzyl radical adds to aromatic systems in the coal structure (requiring subsequent loss of a H-atom or a radical fragment) or, as shown in Scheme 1, that the benzyl radical recombines with the ring carbon of a phenoxy radical, forming (after tautomerization) a moderately refractory hydroxy-substituted diarylmethane linkage. Simple oxygen-centered recombination of the benzyl radical with a phenoxy would not produce a "strong" bond and hence would not lead to a true retrograde product. In either case, the technologically relevant fact that the nonvolatile products have incorporated from 50 to 90% of the grafted groups suggests that the initial yields of light products in coal pyrolysis/gasification or liquefaction could be increased by a factor of 2$-$10 *if* these retrograde reactions could be substantially suppressed.

Pyrolysis of Polymeric Coal Models. Squire and Solomon addressed structure$-$reactivity relationships for coals by synthesizing and then pyrolyzing 27 polymers containing aromatic, hydroaromatic, and heteroaromatic groups linked together by ethylene, methylene, propylene, oxymethylene, ether, aryl$-$aryl, sulfide, and ester bridges.[19$-$21] The primary focus of this research was on two-atom, that is, weak, linkages because the traditional picture of thermal coal conversion chemistry then held that coal conversion resulted from spontaneous thermal cleavage (i.e., homolysis) of such weak linkages. Consequently, there has been some tendency to view the results as basically confirming a correspondence between the rates of thermolysis of weak linkages and the ease of conversion to volatiles. Such correspondence does in fact exist: Most of the polymer models contained weak linkages, and they come apart largely by homolysis of those linkages. As with the studies of Zabransky and Stock, however, the work

Retrograde Products in Coal Conversion

J. Phys. Chem. A, Vol. 110, No. 21, 2006 **6759**

TABLE 2: Char Yields from Pyrolytic Conversion of Various Polymers

Structure	BDE (kcal/mol)	Estimated Homolysis Half-Life at 500°C	Char Yield (wt%)		
			TGA[a]	Heated Grid[b]	Flash Pyrolysis[c]
(1)	54.2	1 s	11.5	4.5	10.9
(9)	57.8	13 s	3.1	5.1	11.0
(12)	43.4	1 ms	27.2	15.4	19.1
(16)	56.4	5 s	6.5	0.5	17.2
(2)	45.1	3 ms	33.3	34.2	22.9
(10)	46.9	11 ms	13.0	3.3	8.1
(27)	57.4	10 s	17.3	--	--

[a] Rate constant estimated using $k = 10^{15.5}e^{-(BDE +1.5)/2.3RT}$. The values for BDE are based on data in refs 22−26. [b] Pyrolysis in a TGA at 30 °C/min with flowing nitrogen to a final temperature of 900 °C. [c] Stainless steel heated grid reactor at 50 °C/s to 500 °C (or 600 °C when marked with an asterisk) and a hold for 20 s. [d] Flash pyrolysis with a heated rate estimated at 1500 °C/s to a final temperature of 1500 °C.

of Squire and Solomon is most revealing for those aspects in which the subjects of study did not simply behave as anticipated.

Pyrolysis data for seven of these polymeric coal models, along with relevant thermochemical values taken from the literature,[22−29] are listed in Table 2. The numbers under the structures refer to those assigned to the polymer by the original authors. The data show that the volatiles yield (1) does not correlate with the weakness of the central bond; (2) decreases with increasing size of the aromatic cluster; (3) increases with donatable hydrogens; and (4) decreases markedly with oxymethylene linkages, notwithstanding C−O bonds that are some 10 kcal/mol weaker than their C−C counterparts. These results, consistent with those for the remaining 20 polymers, very clearly reiterate that retrogressive reactions limit volatile yield, even in the absence of oxygen-containing linkages.

The trend of increasing char yield with increasing cluster size might seem surprising, considering that the strengths of the central bonds decrease substantially through the same series. However, a weaker bond between larger clusters means that homolysis will produce progressively larger aralkyl radical fragments at progressively lower temperatures and vaporization of the capped (or uncapped) fragments before retrogression is given a chance to occur becomes less likely. In addition, radical addition and displacement reactions on aromatic systems become more facile as the size of the ring system increases. The reaction steps are represented in Scheme 2, and the thermochemical factors that control coupling are summarized in Table 3 for some of the ethylene-bridged aromatic and hydroaromatic polymers in this series. Examination of the values in this table, as discussed below, strongly suggests that in this series the

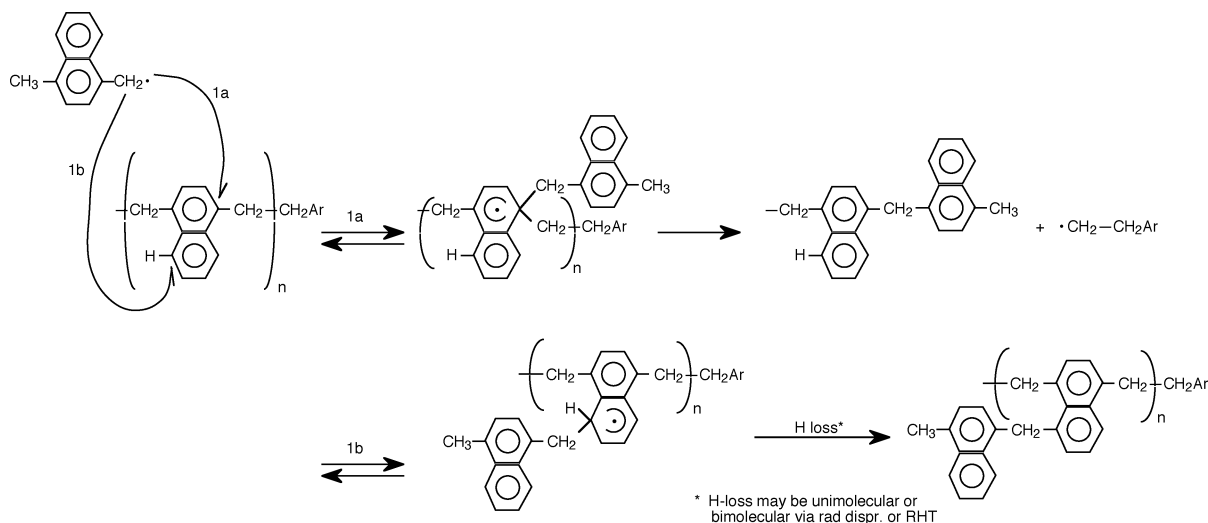**SCHEME 2: Radical Displacement Reactions Leading to Retrograde Products**

TABLE 3: Char Yields and Thermochemical Properties of Various Ethylene-Bridged Arene Polymers

arene	char yield[a] (%)	BDE[b] (kcal/mol)	$t_{1/2}{}^c$ (s, 500 °C)	$\Delta H°$ rad. addn[b] (reacn 1) (kcal/mol)	$T_{1/2}$ adduct reversal[c] (reacn −1) (s, 500 °C)	$t_{1/2}$ formation of stabilized adduct[d] (h, 500 °C) with H-removal by			k coupling/ k homolysis
						H-elim	ArCH$_2$CH$_2$• elim	bimol H-transfer	
benzene	7.1	61	80	−1	3×10^{-11}	5	0.2	2000	0.1
naphthalene	11.5	54	1	−7	2×10^{-9}	20	0.4	40	0.001
benzene, naphthalene	17.3	57	10	-10^e	7×10^{-9}	2	0.06	5	0.05
				$+3^f$	3×10^{-11}	40	2	20 000	0.001
anthracene	27.2	43	0.001	−13	3×10^{-8}	300	2	0.6	0.002
benzene, anthracene	*g*	49	0.037	-22^e	2×10^{-6}	1000	0.008	7 s	0.005
				$+8^f$	1×10^{-11}		700	600 000	1×10^{-5}
tetralin	7.1	58	13	+0,7	5×10^{-11}	10	7	5000	5×10^{-4}
octahydro-anthracene	6.5	56	5	+2	4×10^{-11}	30 000	20	10 000	7×10^{-5}

[a] From refs 19−21; samples heated at 30 °C/min to 900 °C under N$_2$ flow at 1 atm. [b] Taken from thermochemical data in refs 22−27 and 38. [c] Estimated assuming log $k(l/m - s) = 15.5 - (BDE + RT)/2.3RT$. [d] Based on literature thermochemical values and rate data in refs 22−32 and 38. Estimates of overall rates of formation and stabilization of adducts are based on the assumption that the critical period in the temperature-ramped pyrolysis results in each case in ∼1 × 10^{-6} M steady-state concentrations of the respective ArCH$_2$• radicals. [e] For addition of the least stabilized ArCH$_2$• to the Ar forming the most stable adduct. [f] For addition of the most stabilized ArCH$_2$• to the Ar forming the least stable adduct. [g] Not synthesized by Squire and Solomon.

dominant factor in determining char yield is the facility of the aromatic cluster in forming and stabilizing adducts. Not only will the intermediate adducts be formed slightly more readily as the size of the ring system increases,[23,24] but their lifetime before re-elimination of the adding radical will be much longer. Furthermore, contact with other large aromatics that exist within the conversion matrix and are good H-acceptors can facilitate the removal of hydrogen to "lock" the retrograde bond into place.

The estimated $\Delta H°$ values for the addition of aralkyl radicals (formed by weak bond homolysis in the respective polymers) to the most favored position on the aromatic rings of those polymers vary from slightly endothermic to moderately exothermic. In the cases where the polymer has two different types of aromatic units, Table 3 shows two values, the first for addition of the smaller aralkyl radical to the larger arene and the second for the addition of the larger radical to the smaller arene. As the values in row 3 illustrate for polymer 27, the former addition is relatively more favored and the latter less favored than the symmetrical case shown in the row immediately above. Clearly, aralkyl radical addition in the single aromatic ring case (row 1) is not very favored; the addition is essentially thermoneutral (i.e., the adduct has a bond strength very near 0), and the lifetime before reversal at 500 °C amounts to less than 1000 vibrations. In the case of the polycyclic and mixed systems, the adduct

formation is significantly more exothermic. However, the lifetimes before reversal are still very short, only a few microseconds for the most long-lived case shown in the table. Since, in all cases considered in Table 3, estimates of the first-order (or pseudo-first-order) rate constants for H-atom loss from the adducts are less by at least 10^3 than the adduct reversal rate constants, there will be a pre-equilibrium between the reactants and the intermediate adduct, and the rate at which adducts are formed and stabilized will be given by

$$\text{Rate}_{\text{retrograde product formation}} = K_1[\text{R}^•][\text{Ar}]k_2 \qquad (1)$$

where K_1 is the equilibrium constant for adduct formation, R$^•$ is the attacking radical, Ar is the aromatic acceptor, and k_2 is the first-order, or pseudo-first-order, rate constant for H-atom loss. Estimates of k_2 values have been made for stabilization by unimolecular elimination of a H-atom,[22,30] unimolecular elimination of a nonbenzylic primary radical (ArCH$_2$CH$_2$•),[22,31] and bimolecular transfer of H$^•$ from the radical adduct either by radical disproportionation[32,33] or by transfer to a closed-shell aromatic ring (radical hydrogen transfer, or "RHT").[14]

In Table 3, overall estimated half-lives for successful bond formation to the aromatic cluster are given in columns 7−9, based on eq 1 and assuming stabilization by each of the unimolecular routes and by the fastest of the bimolecular routes.

Retrograde Products in Coal Conversion

J. Phys. Chem. A, Vol. 110, No. 21, 2006 **6761**

We emphasize that these estimates are not intended to be "fine" predictions but are to be used to assess whether a particular pathway is orders of magnitude more or less favorable than another, or whether any particular pathway is, by a large margin, unfeasible. Given that qualification, the estimated half-lives offer interesting insights.

First, all of the estimates suggest adduct formation (at 500 °C) should be relatively slow on the coal conversion time scale; only in a few cases do the expected half-lives at 500 °C turn out to be less than 10 min. This estimate seems consistent in general terms with estimates made by Stein and co-workers in the course of their experimental studies on coupling reactions[34,35] but is perhaps a little low to be completely consistent with the observed char yields shown in Table 2.

Inspection of the estimated half-lives for the ethylene-bridged polymers of benzene, naphthalene, and anthracene (rows 1, 2, and 4) shows that if stabilization were to occur via unimolecular loss of an H-atom or a radical, retrograde product formation would become *less* favorable as the size of the aromatic units increases. With increasing size of the aromatic acceptor system, the increased stability of the adduct formed by attack of a given radical is exactly off-set by an identical increase in the difficulty of H-atom or radical loss to form the stable product. However, because aralkyl radicals containing that same polycyclic aromatic hydrocarbon (PCAH) also form weaker bonds with increasing size of the PCAH, the net result is that adduct formation via unimolecular loss of a H-atom or a radical is less favored for the better PCAH acceptor.[23,24] For example, bonds made to the 9-position of An will be ∼21 kcal/mol stronger than those made to a single phenyl ring. However, as the adding species, 9-anthrylmethyl radical forms a bond ∼8 kcal/mol weaker than the benzyl radical does. This combination provides a net strengthening of the adduct by 13 kcal/mol, not enough to compensate for the ultimately required H-loss, which is 21 kcal/mol more difficult from the 9-anthryl adduct.

In contrast, stabilization via bimolecular H-transfer is estimated to become progressively more feasible as the PCAH size increases. This trend is in accord with experimental char yields. These estimates show this trend because the equilibrium constant for the formation of the adduct intermediate increases with increasing size of the aromatic. Removal of an H-atom from the intermediate by RHT will be relatively constant, because this H-transfer is taken to occur in all cases to another molecule of the same PCAH from which the adduct radical is formed and is therefore always thermoneutral. Removal of an H-atom by radical disproportionation also becomes relatively more favorable as the size of the PCAH increases, because there will be little or no activation energy and the radical steady-state populations will increase with increasing PCAH size. Thus, we conclude that retrograde product formation could not be taking place via the addition of resonance-stabilized radicals if unimolecular H-atom loss were the dominant adduct stabilization route. However, stabilized-radical addition, followed by bimolecular H-atom removal, appears to definitely be feasible.

Table 3 also shows estimates for the half-lives of two copolymers (rows 3 and 5). Clearly, the chances of forming a stable retrograde product are enormously increased by the addition of the stronger bond-forming radical (the ArCH$_2^\bullet$ radical with the smaller aryl group) to the PCAH that is the better acceptor, namely, the larger Ar system. Thus, an adduct from a benzyl radical to a naphthalene ring is more likely to be formed and stabilized than those formed in either the pure naphthalene or pure phenyl systems. This expectation is consistent with the higher char yield shown for the copolymer in row 3 in comparison with those for the polymers in either row 1 or 2. The copolymer in row 5, which was not studied by Squire and Solomon, is shown in Table 3 for completeness and because it relates to the anthracene coupling work of Stein, which showed increased coupling rates for cross products.[36,37] The estimated half-life of 7 s for generation of the more favored product from that polymer is in fact the shortest for any of the systems considered here.

The estimated half-life of 36 min for polymer 12 (row 4) is not out of line with the 26% char yield observed by Solomon and Squire in a temperature-programmed pyrolysis lasting 30 min.[21] Thus, the rough correspondence between char yields and estimated retrogression rates in Table 3 leads us to explore further the possibility that bond formation by the addition of resonance-stabilized radicals may play a significant role in char formation from ethylene-bridged polymers and possibly from coal structures in general. Specifically, we note the following:

(1) Adduct stabilization by RCH$_2^\bullet$ elimination or bimolecular H-transfer is always more favorable than adduct stabilization by unimolecular H-elimination.

(2) Completion of the retrograde process by radical elimination tends to be more favorable for smaller aromatic systems; bimolecular H-atom removal becomes relatively more favorable with increasing PCAH size, because the unimolecular loss processes have become more difficult but the bimolecular processes have not.

(3) The estimated rates follow trends in good agreement with the variations in char yields observed for weakly bonded hydrocarbon polymers, and the estimated absolute rates of retrograde product formation appear to be correct within an order of magnitude.

Although the presence of hydroaromatic structures clearly inhibits char formation, one cannot assign with certainty the primary cause of the inhibition by examining the values for the polymers in Table 3. The inhibition could be due to any or all of the following factors: (1) improved radical scavenging, (2) increased induced bond scission (i.e., reversal of retrograde reactions), (3) decreased ability to stabilize adducts, and disfavored adduct formation with the smaller π-systems of the hydroaromatic clusters.

The relative importance of these factors is difficult to intuit and is best addressed using a mechanistic numerical model of conversion that incorporates the various reactions indicated by the foregoing analysis.

Mechanistic Numerical Modeling

General Approach. We used a mechanistic numerical model, very similar to one we used previously to address major coal cleavage processes,[14] to address retrograde reactions that occur via the addition of resonance-stabilized radicals to aromatic ring systems. We chose the addition of stabilized radicals as a stand-in for retrogressive reactions not because we believe it to necessarily always be the most important class but because it is the class of bond-making reactions whose outcome is most likely to be sensitive to the changing of various H-transfer rates. As discussed above, the addition of resonance-stabilized radicals is highly reversible, such that if it results in successful formation of strong bonds between aromatic clusters, it will be because a very small fraction of a large number of original additions ultimately go on to stable products. In contrast, the addition of aryl radicals (once generated) will be rapid and essentially irreversible in the condensed-phase medium present in the early stages of conversion. Hence, resonance-stabilized-radical addition is the coupling process whose outcome can vary the most

widely, and which we therefore thought it would be most informative to address.

The model we have used is very detailed; it incorporates all fundamental chemical reactions of all closed-shell and free-radical species that were judged to be significant. Because of this detail, the model, of necessity, includes only a very limited set of starting structures. In many cases, the "coal" is represented by only three hydrocarbon structures, together with H_2 or some other additive. Since there are no heteroatom-containing structures, only reactions operating through uncharged free radicals are included. Even so, this limited set led to product mixtures containing 45 species and 172 reactions, after eliminating some of the reactions that were found to be unimportant.

With so many reactions, it is easy for the modeling effort to deteriorate into a parameter-fitting exercise. To guard against that, we adopted a strict regimen for selecting the activation energies and *A*-factors based on the known thermochemical properties of the species.[14] In cases where the thermochemistry of the species was not known, we used the group-additivity rules of Benson, Golden, and their co-workers to arrive at the parameters.[22] The reactions and rate parameters used in the model are shown in Table 4. Table 5 lists thermochemical values and sources for the species used in the modeling. The identities of the major species are shown in Scheme 3, except for the solvent species F0, F9, and F10H, which represent phenanthrene, 9-hydrophenanthryl radical, and 9,10-dihydrophenanthrene, respectively, and A0, A9, and A10H for the corresponding species in the anthracene system.

Methodology and Simplifying Assumptions. The model is homogeneous: it consists of relatively low-molecular-weight species assumed to be miscible in all proportions, free of concentration gradients, and requiring no mass or heat transport. These are obviously gross simplifications, leaving out various transport factors that ultimately can have a marked impact on the chemistry. However, the discussion of coal conversion mechanisms has to date been conducted in the realm of the chemical reactions themselves. The model was *not* intended in any way to actually predict the conversion of a real coal but was simply intended to explore how chemical factors influence certain classes of reactions under different circumstances. Thus, we begin by examining the baseline provided by the chemistry itself but comment where appropriate on the probable impact of the simplifying assumptions.

Among the factors that come into play in the liquefaction of a real coal is the effect of viscosity on cage recombination. Stein and co-workers have addressed the effect of cage recombination on bibenzyl decomposition by comparing the rates observed in the gas phase, in liquid tetralin, and in liquid dodecahydro-triphenylene, the tetracyclic analogue of tetralin.[38] At 400 °C, the rates in liquid dodecahydrotriphenylene and tetralin are slowed moderately, to 46 and 73%, respectively, of the gas-phase value. The liquid-phase rates in tetralin essentially coalesce with the gas-phase rates at the critical point of tetralin, 444 °C.

Our previous measurements on the liquefaction of poly(1,4-dimethylenenaphthalene),[9] the polymeric version of the dimeric coal model that we use in this modeling study, offer an instructive comparison with the work of Stein. We found the hydrogenolysis (displacement by H-atom attack) and perhaps also radical attack at the ipso positions of the naphthalene rings in dihydrophenanthrene or dihydroanthracene solvents to be roughly competitive with homolysis of the weak central bonds. Our measured rates of hydrogenolysis and homolysis represent about a 10-fold increase and a 30-fold decrease, respectively,

compared to the rates measured for dimeric analogues in the gas phase. The 10-fold slowing of homolysis in the polymer was qualitatively consistent, but decidedly greater, than the roughly 2-fold slowing reported by Stein for bibenzyl itself. This increase in attenuation is perhaps not surprising for a polymer having a number average molecular weight of about 10 000 Da.

The 10-fold increase in hydrogenolysis relative to a dimeric substrate can be rationalized in the following manner. First, reversal of hydrogenolysis is less likely than cage recombination of two radicals, because the former involves a radical addition process with an activation energy of 7−10 kcal/mol, while the latter is an essentially zero-activation-energy recombination. Second, diffusional limitations could benefit hydrogenolysis: after scavenging a homolytically produced polymeric radical, a dihydroaromatic solvent molecule is converted into a H-atom-bearing cyclohexadienyl radical in the immediate vicinity of the polymer backbone, resulting in an enhanced rate of H-transfer to bring about hydrogenolysis. Evidence for such enhancement can be found in the pyrolysis of silica-supported bibenzyl.[39]

Leaving rationalizations of the cage effects and other diffusional effects aside, the observations reported in the paragraphs above are entirely consistent with the fact that the numerical model based on unadjusted, experimentally based, gas-phase rate parameters will likely over-represent homolyses and under-represent displacement reactions. Indeed, in the current model, it was only after we made addition to the naphthalene ring system 4 kcal/mol more favorable than accepted gas-phase thermochemical data would dictate—an adjustment that reflects better acceptor species and a resultant increase in the steady-state concentration of adduct intermediates of about an order of magnitude than the gas-phase value—that we saw comparable yields of radical displacement products (both retrogressive and "progressive"). This result also conforms more closely to our measured values[9] for hydrogenolysis of poly(1,4-dimethylene-naphthalene) in a moderately viscous donor solvent.

Reaction Sequence. Our coal surrogate consists of two naphthalene rings joined by a weak bibenzyl-type linkage, chosen not because it is thought to represent the cleavable linkages in any particular coal but because it undergoes homolysis on time scales roughly consistent with observed coal conversion rates and allows us to examine how the aralkyl radicals react via radical displacement reactions. Furthermore, dinaphthylethane is the dimeric analogue of the polymer whose pyrolytic behavior was experimentally studied by Squire and Solomon[21] and whose liquefaction behavior we subsequently examined.[9] In addition, beginning with a surrogate in which there are no intercluster connections that consist *exclusively* of strong bonds tends to draw more attention to the strong linkages (i.e., retrograde products) that are generated during the course of reaction.

Scheme 3 shows the major reaction types and species generated during reaction alone or with added H_2. In this simplified picture, the linked clusters in coal are represented by 1,2-(1,1′-dinaphthyl)ethane (labeled MN2), and smaller amounts of 9,10-dihydrophenanthrene and phenanthrene, or 9,10-dihydroanthracene and anthracene, are used to represent the hydrogen donors and acceptors either present in coals or added as liquefaction solvent components. To illustrate the benefit from H_2 or additional donors, the model was typically operated with low hydroaromatic content so as to represent either pyrolysis/gasification or liquefaction conditions in which the concentration of H-donors is a major limiting factor.

Retrograde Products in Coal Conversion

J. Phys. Chem. A, Vol. 110, No. 21, 2006 **6763**

TABLE 4: Reaction Sequence for Coal Surrogate Bond Cleavage and Retrogression

reacn no.	reactants	products	A-factor	activation energy	reacn type	reacn no.	reactants	products	A-factor	activation energy	reacn type
1	F10, HF0	F9 F9	0.348×10^{10}	0.250×10^5	RRD	70	NMNM	MN− MN	0.631×10^{14}	0.126×10^5	R-elim
2	F9, F9	F10HF0	0.264×10^{10}	0.463×10^2	RD	71	NMNM	NMN CH$_3$	0.631×10^{14}	0.160×10^5	R-elim
3	MN2, F0	MN2−F9	0.348×10^{10}	0.245×10^5	RRD	72	NMN, CH$_3$	NMNM	0.150×10^9	0.338×10^4	R-addn
4	MN2, −F9	MN2 F0	0.132×10^{10}	0.157×10^3	RD	73	MN3, F0	MN2−F9	0.348×10^{10}	0.245×10^5	RRD
5	MN, F0	F9 MN−	0.261×10^{10}	0.263×10^5	RRD	74	MN2−, F9	MN3 F0	0.132×10^{10}	0.157×10^3	RD
6	MN−, F9	MN F0	0.132×10^{10}	0.000×10^0	RD	75	CH$_3$, N	HMN	0.600×10^9	0.338×10^4	R-addn
7	F9, MN2	HMN2F0	0.280×10^9	0.834×10^4	RHT	76	CH$_3$, MN3	MN2M	0.300×10^9	0.338×10^4	R-addn
8	HN2	HMN2	0.400×10^{11}	0.136×10^4	H-addn	77	EN, H	ENH	0.200×10^{11}	0.137×10^4	H-addn
9	F9, MN	HMN F0	0.140×10^9	0.834×10^4	RHT	78	ENH	EN H	0.450×10^{14}	0.176×10^5	H-elim
10	H$_2$, MN−	H MN	0.100×10^{11}	0.135×10^5	H-abs	79	EN, F9	ENH F0	0.140×10^9	0.835×10^4	RHT
11	MN, H	MN− H$_2$	0.810×10^{10}	0.438×10^4	H-abs	80	ENH, F0	EN F9	0.140×10^9	0.828×10^4	RHT
12	H, F10H	H$_2$ F9	0.108×10^{12}	0.404×10^4	H-abs	81	EN, MN2−	ENH STLB	0.140×10^9	0.108×10^5	RHT
13	H$_2$, F9	H F10H	0.100×10^{11}	0.146×10^5	H-abs	82	ENH, STLB	EN MN2−	0.140×10^9	0.694×10^4	RHT
14	MN2−, F10H	MN2 F9	0.400×10^9	0.844×10^4	R-abs	83	ENH	N E−	0.631×10^{14}	0.150×10^5	R-elim
15	MN2, F9	MN2−F10H	0.200×10^9	0.784×10^4	R-abs	84	N, E−	ENH	0.600×10^9	0.374×10^4	R-addn
16	F9	F0 H	0.900×10^{14}	0.177×10^5	H-elim	85	ENH, F9	EN F10H	0.660×10^9	0.333×10^2	RD
17	F0, H	F9	0.400×10^{11}	0.136×10^4	H-addn	86	ENH, MN−	EN MN	0.660×10^9	0.000×10^0	RD
18	F9, MN3	F0 HMN2	0.280×10^9	0.834×10^4	RHT	87	CH$_4$, H	CH$_3$ H$_2$	0.108×10^{12}	0.701×10^4	H-abs
19	F9, HMN2	MN2 F10H	0.660×10^9	0.370×10^2	RD	88	CH$_3$, H$_2$	CH$_4$ H	0.100×10^{11}	0.656×10^4	H-abs
20	HMN2	N EN−	0.631×10^{14}	0.150×10^5	R-elim	89	CH$_4$, MN−	CH$_3$ MN	0.400×10^9	0.141×10^5	M-abs
21	EN−, F10H	EN F9	0.400×10^9	0.510×10^4	R-abs	90	CH$_3$, MN	CH$_4$ MN−	0.300×10^9	0.448×10^4	M-abs
22	EN−, MN2	EN MN2−	0.400×10^9	0.489×10^4	R-abs	91	E, F9	E− F10H	0.300×10^9	0.135×10^5	R-abs
23	MN, EN−	MN− EN	0.300×10^9	0.558×10^4	R-abs	92	CH$_4$, F9	CH$_3$ F10H	0.400×10^9	0.151×10^5	M-abs
24	HMN2, F0	MN2 F9	0.140×10^9	0.829×10^4	RHT	93	CH$_3$, F10H	CH$_4$ F9	0.400×10^9	0.414×10^4	M-abs
25	HMN, F0	MN F9	0.140×10^9	0.829×10^4	RHT	95	E−, F10H	E F9	0.400×10^9	0.511×10^4	R-abs
26	CH$_3$, MN2	MN2M	0.300×10^9	0.338×10^4	R-addn	96	E−, CH$_4$	E CH$_3$	0.400×10^9	0.972×10^4	R-abs
27	MN2, M	CH$_3$ MN2	0.631×10^{14}	0.160×10^5	R-elim	97	CH$_3$, E	CH$_4$ E−	0.135×10^{12}	0.603×10^4	R-abs
28	MN−, F10H	MN F9	0.400×10^9	0.758×10^4	R-abs	99	E, H	E− H$_2$	0.162×10^{12}	0.614×10^4	H-abs
29	F9, MN	MN− F10H	0.300×10^9	0.894×10^4	R-abs	100	E−, MN2	E MN2−	0.400×10^9	0.490×10^4	R-abs
30	CH$_4$, MN2−	CH$_3$ MN2	0.400×10^9	0.156×10^5	M-abs	101	E, MN2−	E− MN2	0.600×10^9	0.139×10^5	R-abs
31	CH$_3$, MN2	CH$_4$ MN2−	0.400×10^9	0.399×10^4	M-abs	102	E−, MN3	E MN2−	0.200×10^9	0.490×10^4	R-abs
32	CH$_3$, MN3	CH$_4$ MN2−	0.400×10^9	0.399×10^4	M-abs	103	HMN, MN−	MN MN	0.660×10^9	0.000×10^0	RD
33	MN2	MN− MN−	0.300×10^{16}	0.287×10^5	thermol	104	MN, MN	HMN MN−	0.261×10^{10}	0.263×10^5	RRD
34	MN−, MN−	MN3	0.300×10^{10}	0.000×10^0	recomb	105	MN−, EN	ENMN	0.150×10^9	0.453×10^4	R-addn
35	HMN	N CH$_3$	0.631×10^{14}	0.160×10^5	R-elim	106	EN, MN	MN− EN	0.631×10^{14}	0.126×10^5	R-elim
36	MN3	MN− MN−	0.300×10^{16}	0.287×10^5	thermol	107	EN, MN	NMN E−	0.631×10^{14}	0.150×10^5	R-elim
37	H, MN	HMN	0.200×10^{11}	0.136×10^4	H-addn	108	NMN, E−	ENMN	0.150×10^9	0.374×10^4	R-addn
38	H, MN3	HMN2	0.400×10^{11}	0.136×10^4	H-addn	109	HMN, F9	MN F10H	0.660×10^9	0.370×10^2	RD
39	MN2M	MN EN−	0.631×10^{14}	0.150×10^5	R-elim	110	MN, F10H	HMN F9	0.174×10^{10}	0.250×10^5	RRD
40	MN−, MN2	M2MN	0.300×10^9	0.453×10^4	R-addn	111	HMN	MN H	0.450×10^{14}	0.176×10^5	H-elim
41	MN, EN−	MN2M	0.300×10^9	0.371×10^4	R-addn	112	HMN, STLB	MN MN2−	0.140×10^9	0.695×10^4	RHT
42	MN−, N	NMNH	0.120×10^{10}	0.453×10^4	R-addn	113	MN, MN2−	HMN STLB	0.140×10^9	0.108×10^5	RHT
43	F9, HMN	F10HMN	0.660×10^9	0.370×10^2	RD	114	EN, MN	ENH MN−	0.131×10^{10}	0.263×10^5	RRD
44	NMNH	MN− N	0.631×10^{14}	0.126×10^5	R-elim	115	EN, F10H	ENH F9	0.174×10^{10}	0.250×10^5	RRD
45	NMNH	NMN H	0.450×10^{14}	0.176×10^5	R-elim	116	E, MN−	E− MN	0.300×10^9	0.126×10^5	R-abs
46	NMN, H	NMNH	0.400×10^{11}	0.136×10^4	H-addn	117	E−, MN	E MN−	0.300×10^9	0.559×10^4	R-abs
47	NMNH, F9	NMN F10H	0.660×10^9	0.370×10^2	RD	118	CH$_3$, EN	CH$_4$ ENP−	0.200×10^9	0.436×10^4	M-abs
48	M2MN	MN− MN2	0.631×10^{14}	0.126×10^5	R-elim	119	CH$_4$, ENP−	CH$_3$ EN	0.400×10^9	0.145×10^5	M-abs
49	NMN, HMN−	NMN MN	0.660×10^9	0.000×10^0	RD	120	E−, EN	E ENP−	0.200×10^9	0.542×10^4	R-abs
50	MN−, MN2	MN MN2−	0.400×10^9	0.737×10^4	R-abs	121	E, ENP−	E− EN	0.300×10^9	0.129×10^5	R-abs
51	MN, MN2−	MN− MN2	0.300×10^9	0.933×10^4	R-abs	122	N, CH$_3$	HMN	0.600×10^9	0.338×10^4	R-addn
52	MN2−	H STLB	0.900×10^{14}	0.211×10^5	H-elim	123	HMN, MN2−	MN MN2	0.660×10^9	0.148×10^3	RRD
53	H, STLB	MN2−	0.400×10^{11}	0.927×10^3	H-addn	124	MN, MN2	HMN MN2−	0.174×10^{10}	0.245×10^5	RRD
54	F9, STLB	MN2−F0	0.280×10^9	0.697×10^4	RHT	125	ENH, MN2−	EN MN2	0.660×10^9	0.144×10^3	RD
55	MN2−, F0	F9 STLB	0.280×10^9	0.108×10^5	RHT	126	EN, MN2	ENH MN2−	0.174×10^{10}	0.245×10^5	RRD
56	MN2−, MN2	STLBHMN2	0.280×10^9	0.108×10^5	RHT	127	NMN, HMN2−	NMN MN2	0.660×10^9	0.148×10^3	RD
57	MN−, MN3	M2MN	0.300×10^9	0.453×10^4	RRD	128	NMN, MN2	NMNHMN2−	0.174×10^{10}	0.245×10^5	RRD
59	MN2−,F9	STLBF10H	0.132×10^{10}	0.750×10^3	RD	129	NMN, F10H	NMNHF9	0.348×10^{10}	0.250×10^5	RRD
60	H, MN2	H$_2$ MN2−	0.108×10^{12}	0.389×10^4	H-abs	130	NMN, MN	NMNHMN−	0.131×10^{10}	0.263×10^5	RRD
61	H$_2$, MN2−	H MN2	0.100×10^{11}	0.150×10^5	H-abs	131	E−, MN2	MN2E	0.300×10^9	0.371×10^4	R-addn
62	M2MN	NMN EN−	0.631×10^{14}	0.150×10^5	R-elim	132	MN, 2E	E− MN2	0.631×10^{14}	0.150×10^5	R-elim
65	H, MN3	H$_2$ MN2−	0.108×10^{12}	0.389×10^4	H-abs	133	MN, 2E	EN EN−	0.631×10^{14}	0.151×10^5	R-elim
66	NMN, EN−	M2MN	0.300×10^9	0.371×10^4	R-addn	134	EN, EN−	MN2E	0.150×10^9	0.369×10^4	R-addn
67	NMN, HF0	NMN F9	0.700×10^8	0.829×10^4	RHT	135	ENP, −MN2	M2EN	0.150×10^9	0.491×10^4	R-addn
68	NMN, F9	NMNHF0	0.140×10^9	0.834×10^4	RHT	136	M2, EN	ENP−MN2	0.631×10^{14}	0.114×10^5	R-elim
69	MN−, MN	NMNM	0.150×10^9	0.453×10^4	R-addn	137	M2, EN	NMMNEN−	0.631×10^{14}	0.150×10^5	R-elim

TABLE 4 (Continued)

reacn no.	reactants	products	A-factor	activation energy	reacn type	reacn no.	reactants	products	A-factor	activation energy	reacn type
138	NMM, NEN−	M2EN	0.150×10^9	0.371×10^4	R-addn	157	CHO, MN−	CO MN	0.660×10^9	0.000×10^0	RD
139	E−, MN3	MN2E	0.300×10^9	0.371×10^4	R-addn	158	MN2, −MN2−	MN2 STLB	0.264×10^{10}	0.861×10^3	RD
141	MEOH, MN−	−MOHMN	0.300×10^9	0.106×10^5	R-abs	159	MN2, STLB	MN2−MN2−	0.348×10^{10}	0.213×10^5	RD
142	−MOH, MN	MEOHMN−	0.300×10^9	0.666×10^4	R-abs	160	MN−, MN2−	MN STLB	0.132×10^{10}	0.500×10^3	RD
144	−MOH, F10H	MEOHF9	0.400×10^9	0.619×10^4	R-abs	161	MN, STLB	MN− MN2−	0.261×10^{10}	0.229×10^5	RD
145	MEOH, MN2−	−MOHMN2	0.300×10^9	0.119×10^5	R-abs	162	MN−, H2O	MN OH	0.870×10^9	0.183×10^5	OH-abs
146	−MOH, MN2	MEOHMN2−	0.400×10^9	0.597×10^4	R-abs	163	MN, OH	MN− H2O	0.198×10^{10}	0.155×10^4	OH-abs
147	−MOH	CH2OH	0.450×10^{14}	0.170×10^5	R-elim	164	F9, H2O	F10HOH	0.870×10^9	0.194×10^5	OH-abs
148	−MO, HMN2	CH2OHMN2	0.140×10^9	0.806×10^4	RHT	165	F10, HOH	F9 H2O	0.264×10^{10}	0.130×10^4	OH-abs
149	−MO, HMN	CH2OHMN	0.700×10^8	0.806×10^4	RHT	166	OH, MN2	H2O MN2−	0.264×10^{10}	0.119×10^4	OH-abs
150	CH2O, MN−	CHO MN	0.200×10^9	0.838×10^4	R-abs	167	H2O, MN2−	OH MN2	0.870×10^9	0.199×10^5	OH-abs
151	CH2O, F9	CHO F10H	0.200×10^9	0.926×10^4	R-abs	168	OH, H2	H2O H	0.132×10^{10}	0.323×10^4	OH-abs
152	CHO, F10H	CH2OF9	0.400×10^9	0.740×10^4	R-abs	169	H2O, H	OH H2	0.870×10^9	0.108×10^5	OH-abs
153	CH2O, MN2−	CHO MN2	0.200×10^9	0.966×10^4	R-abs	170	OH, N	H2O N−	0.528×10^{10}	0.377×10^4	OH-abs
154	CHO, MN2	CO HMN2	0.140×10^9	0.533×10^4	RHT	171	H2O, N−	OH N	0.870×10^9	0.845×10^4	OH-abs
155	CHO, MN	CO HMN	0.700×10^8	0.533×10^4	RHT	172	N−, N	NNH	0.132×10^{10}	0.241×10^4	aryl-addn
156	CHO	CO H	0.450×10^{14}	0.101×10^5	H-elim						

As shown in Scheme 3, MN2 can react by weak bond homolysis and via displacement by H-atoms, either free or transferred directly from closed-shell or radical H-carrier species, and can also react through displacement by methyl, ethyl, arylmethyl, and 2-arylethyl radicals. The radicals formed in these reactions can be scavenged by hydrogen transfer from di-hydrophenanthrene, from the aliphatic hydrogens on MN2 itself, from any of the alkyl-aromatic reaction products (e.g., methyl- and ethyl-naphthalene), or from H_2 or other added reagents. (For simplicity's sake, Scheme 3 does not explicitly show H-atom sources for either scavenging of hydrogenolysis.) The "true" retrograde product in this scheme is considered to be the dinaphthylmethane species, labeled NMN. The principal initial route to the formation of NMN is found from the results of the modeling to involve attack of the naphthylmethyl radical (MN−) on MN2 to yield the intermediate adduct M2MN, which is stabilized by unimolecular loss of the 2-phenethyl radical (EN−).

Recombination of the initial homolysis fragments regenerates MN2, which for purpose of tracking the extent of recombination is labeled MN3. MN3 is allowed to react in all ways like MN2; when various displacement intermediates are produced from MN3, they lose their label and become identical to those generated from MN2. Reversal of the addition reactions that gave these intermediates results in regeneration of MN2, providing a route back from the labeled species MN3.

The initiation processes include not only homolysis of MN2 (and MN3) but also reverse radical disproportionation (RRD) between various benzylic C−H bonds and various aromatics (i.e., the major naphthalene and phenanthrene or anthracene species).[40] One of the principal simplifying assumptions is that no di- or tetra-hydronaphthalene or tetra-hydrophenanthrene species are produced by successive hydrogen transfers. Previous experimental[4,7] and modeling[14] studies have shown that this assumption is much more nearly correct when the system is relatively poor in hydroaromatics, as it typically was in the cases studied here (the dihydrophenanthrene/phenanthrene ratio was usually 0.1 M/0.5 M).

Reaction Simulation Conditions. For the most part, the model was designed to mimic coal liquefaction conditions with a solvent-to-coal ratio of 1:2 (i.e., solvent-poor conditions). Accordingly, as a starting point, we used a total concentration of about 3 M for species of MW around 200. The typical concentration of the starting coal (i.e., MN2) was set at 0.7 M;

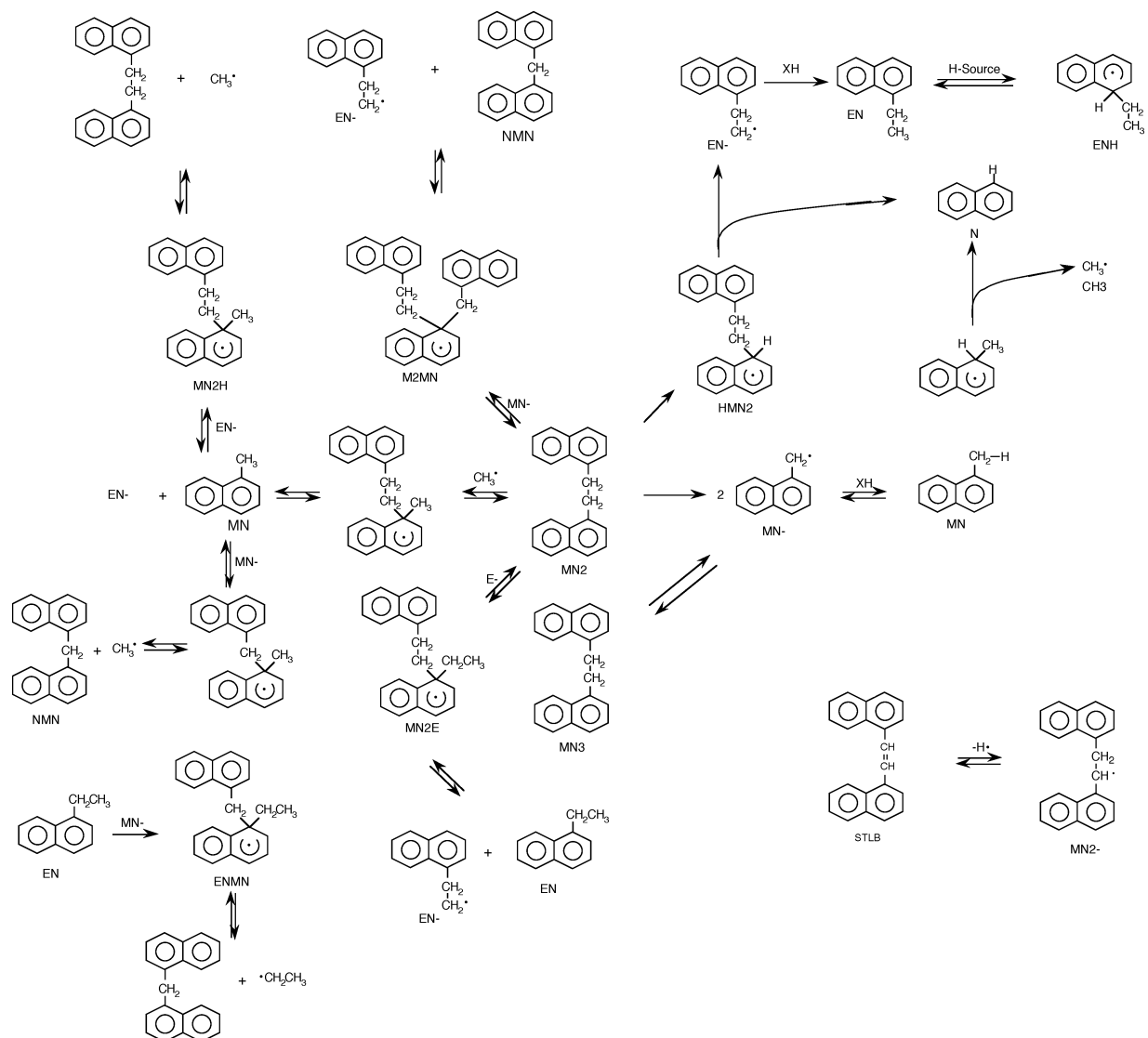**TABLE 5: Heats of Formation for Species Used in the Numerical Model**

species[a]	$\Delta H°_{f,298}$[b] (kcal·mol)	species[a]	$\Delta H°_{f,298}$[b] (kcal·mol)
F0	50.0	MN3	66.2
F9	68.3	EN	23.1
F10H	37.1	HMN2	84.6
A0	55.2	MN2M	76.2
A9	63.8	NMN	63.3
A10H	38.2	NMNH	81.7
MN	27.7	NMNM	73.3
MN−	61.6	H_2	0.0
HMN	46.1	H	52.1
M2MN	111.8	N	36.1
E−	27.7	MN2	66.2
ENH	41.5	CH_4	−17.9
E	−20.2	CH_3	35.1
ENMN	68.7	MEOH	−48.0
MN2E	71.4	−MOH	−6.2
M2EN	109.2	OH	9.4
NMMN	60.7	CH_2O	−26.0
H_2O	−57.8	CHO	8.9
N−	94.0	CO	−26.4
NNH	106.1	MN2−	96.2
NN	76.0	EN−	71.0
C2H6	−20.2	ENP-	56.0
STLB	85.5		

[a] Species identities are as shown in Scheme 3. [b] Measured heats of formation are from refs 22−24, 28, 29, 31, and 35. In certain cases, such as HDNM, the cyclohexadienyl radical produced by H-atom transfer to the 1-position (ipso) of dinaphthylmethane, the heat of formation is for the unsubstituted radical. This amounts to the zeroth-order assumption that group additivity holds for the reactions being considered, i.e., that substitution *not* at sites having significant odd electron density upon H-transfer does not affect the thermodynamics and kinetics of the H-transfer significantly.

the aromatic content in the solvent (F0 or A0) was 0.5 M, and the dihydroaromatic (F10H or A10H) was between 0.1 and 2.0 M. This was designed to mimic conditions such as mild gasification (low "solvent") or liquefactions in solvents with high donor content. The activity of H_2 in solution is taken as being equal to that provided by presumed equilibrium with the gas-phase H_2 pressure (1000 psi cold), under conditions of very limited H_2 supply (i.e., essentially zero headspace in a batch reactor).

The model was operated in an isothermal manner, at 400, 500, and 600 °C, for reaction times generally of 8000, 64, and 64 s, respectively. These temperatures and times were chosen

Retrograde Products in Coal Conversion

J. Phys. Chem. A, Vol. 110, No. 21, 2006 **6765**

SCHEME 3: Major Species and Reaction Types Included in the Conversion Model

H-Atom Sources: H_2, H•, PhenH$_2$, PhenH•, MN2⁻

to cover the range in which real coals, as well as this model, undergo rapid and widespread radical reactions under not only liquefaction but also pyrolysis conditions. At all but the most rapid heating rates, they represent the range over which coals become fluid, evolve the bulk of the moderate-molecular-weight volatiles that are produced, and undergo substantial solidification to a char that is then much less easily converted to liquids or moderate-molecular-weight volatiles. Hence, the chemistry that occurs in this temperature regime is important in itself as well as in determining the nature of the char that must be subsequently gasified. When the temperature is increased from 400 to 500 °C, the total reaction time is shortened from 8000 to 64 s to provide a similar fractional reaction. At 600 °C, only 2 s is required to yield a similar fractional reaction, but the model was still run to 64 s in order to cover the range of reaction times relevant to various gasification processes.

The simulations were performed on a VAX 11/750 computer using OLCHEM, a numerical integration routine based on the Gear algorithm that automatically adjusts the step size to accommodate varying degrees of stiffness. The results of computations using this model are illustrated primarily using area graphs to depict the evolution of various products as a function of time.

Results of the Modeling

Product Groupings. We generally present the results in terms of the following product groups, typically listed from lighter ("most converted") to heavier ("least converted" or retrograde):

(1) Strong bond cleavage: naphthalene (N) and ethylnaphthalene (EN), from H-atom displacement and radical displacement reactions

(2) Weak bond cleavage: methylnaphthalene (MN)

(3) Functioning of the starting material as hydrogen donor: dinaphthylethylene (STLB), the stilbene analogue from the loss of two H's from an intact C_2 bridge.

(4) Displacement by a naphthylmethyl radical: dinaphthylmethane (NMN), a true retrograde product

(5) Radical recombination: dinaphthylethane (MN3), a temporary retrograde product

(6) Starting material: dinaphthylethane (MN2)

Effect of Scavenger Structure. Examination of the impact of changing scavenger type illustrates two factors that have widespread implications. These are the following: (1) All scavengers that operate via a radical capping process have a dual role—they also act as chain transfer agents and sometimes as actual initiators via the reverse of radical disproportionation.[40]
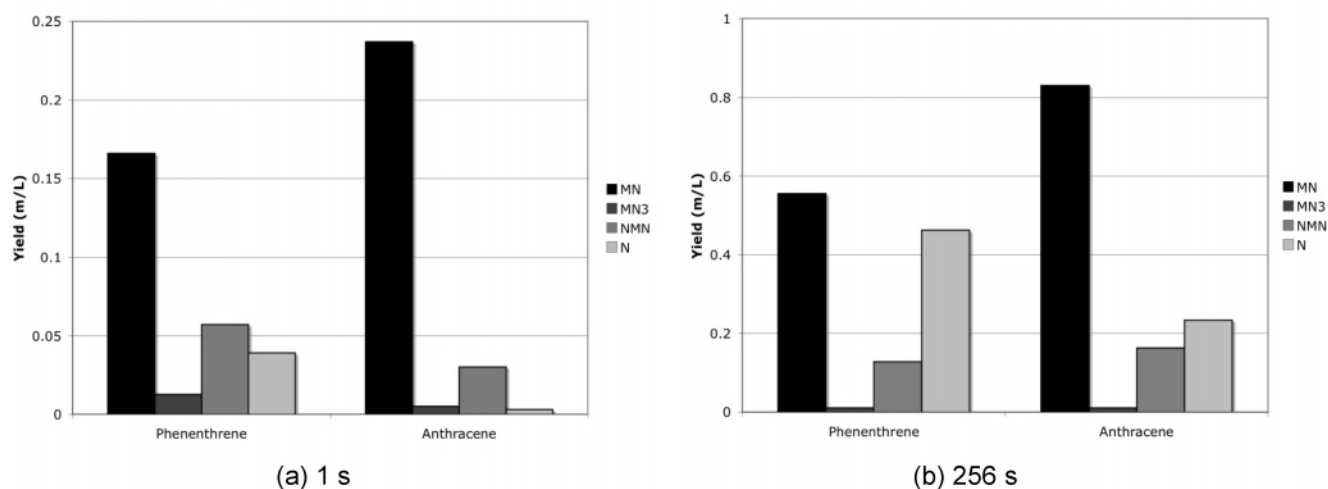
6766 *J. Phys. Chem. A, Vol. 110, No. 21, 2006*

McMillen and Malhotra

Figure 1. Computed yields of products resulting from radical capping, recombination, displacement, and hydrogenolyis for two scavenger types at 500 °C and short and long reaction times. Substrate MN2, 0.7 M; hydroaromatic, 2.0 M; aromatic, 0.5 M.

(2) "Scavengers" typically found to best aid coal conversion to volatiles or liquids appear to perform better because they are superior in some aspect *other* than scavenging. Figure 1 shows computed yields of the scavenged fragment methylnaphthalene, the recombination product MN3, the true retrograde product NMN, and the hydrogenolysis product naphthalene, produced when the coal surrogate is allowed to react in the presence of an excess of two different hydroaromatics for short and long reaction times. One of these hydroaromatics is 9,10-dihydro-phenanthrene, which has been used as the representative of the native hydroaromatic structures in coal in the rest of the modeling results presented here. The other is 9,10-dihydro-anthracene, which is isomeric with dihydrophenanthrene but is well-known to be a much better radical scavenger, because the 9,10 C−H bonds are about 6 kcal/mol weaker than those in dihydrophenananthrene.[41] This lower bond strength means that at 500 °C radical capping will occur roughly an order of magnitude faster with dihydroanthracene. The computed product yields show that, at short reaction times (1 s), where there is a large generation of fragment radicals from homolysis of the weakly bonded coal surrogate, dihydroanthracene indeed maximizes the yield of capped fragment radicals (MN) and minimizes the yield of recombination product MN3 and retrograde product NMN. However, at long reaction times (256 s), the yield of retrograde product NMN is actually higher in dihydroanthracene, the "better" scavenger.

Examination of the individual reaction fluxes at longer reaction times when the burst of radicals from the decomposing coal has largely died away shows that the principal source of fragment radicals is then abstraction of hydrogen atoms from the previously capped fragment species MN by the pool of scavenger radicals generated by the scavenger itself. Under these conditions, the retrogression actually becomes worse in the presence of the better scavenger, such that the generation of the retrograde product NMN becomes fast enough to eventually overtake that observed in the poorer scavenger system. The differences illustrated in Figure 1 may not appear large, but when the instantaneous rates are examined, one finds that not only does the rate of NMN formation in the presence of dihydroanthracene substantially exceed that in dihydrophenan-threne, but also the rate in dihydrophenanthrene is negative. That is, in dihydrophenenthrene, at longer reaction times, the rate of hydrogenolysis of the retrograde product exceeds the rate of its formation, and the fractional yield of cleaved products improves at long reaction times. In contrast, in the better

scavenger, it continues to get worse. Thus, the model elaborates a trend which has been noted previously, namely, that coal conversion tends to be better in the presence of hydroaromatics that are *not* the better scavengers,[7] and is evidently better because these latter scavengers tend to be better hydrogenolysis reagents.

Effect of Added H_2. Figure 2 contains six panels showing the simulated evolution of stable products containing one or more naphthalene rings. The three on the left are for runs at 400, 500, and 600 °C in solvent with low donor content and with no added hydrogen, while those on the right correspond to runs in the same solvent but with 1000 psi H_2. In each graph, the higher-molecular-weight products (STLB, NMN, MN3, and MN2) are at the bottom and the products representing conversion (i.e., containing only one naphthalene ring; N, EN, MN) are at the top. The data suggest increasing the temperature from 400 to 500 °C causes little increase in the fractional yield of cleaved products (N, EN, MN). Increasing the temperature to 600 °C actually causes a *decrease* in the sum of cleaved products present at the end of each reaction time, as shown in Table 6. However, this table does show that at 600 °C the fractional yield of cleaved products present at the end of the time required to achieve a similar fractional decomposition (i.e., ∼2 s) does rise slightly from 500 °C; it is when reaction is allowed to continue for 60 s that the fractional yield of cleaved products declines to approximately half its maximum value! Thus, we see that increasing temperature provides more reaction, but if there is not something to mitigate retrograde reactions, higher temper-atures tend to cause the retrograde reactions to increase as fast or faster than the bond-cleavage reactions. This modeling result appears to be completely in accord with the common observation that higher heating rates tend to decrease char yields in coal pyrolysis only when accompanied by rapid removal of volatile products.[42,43] This agreement is satisfying, since there has been absolutely no attempt to make the model correspond to the phenomenology of coal pyrolysis; more importantly, the agree-ment suggests that other trends elaborated by the model may have some significance for the pyrolysis of real coals.

The impact of H_2 is rather modest at 400 °C, progressively more important with increasing temperatures, and is strikingly pronounced at 600 °C. As Table 6 shows, at this temperature, 1000 psi H_2 decreases the percent uncleaved from 75 to 23%, but the changes are much smaller at 500 and 400 °C, and even much less significant at 600 °C if the reaction time is held to the 2 s that results in fractional homolysis similar to the 64 s at
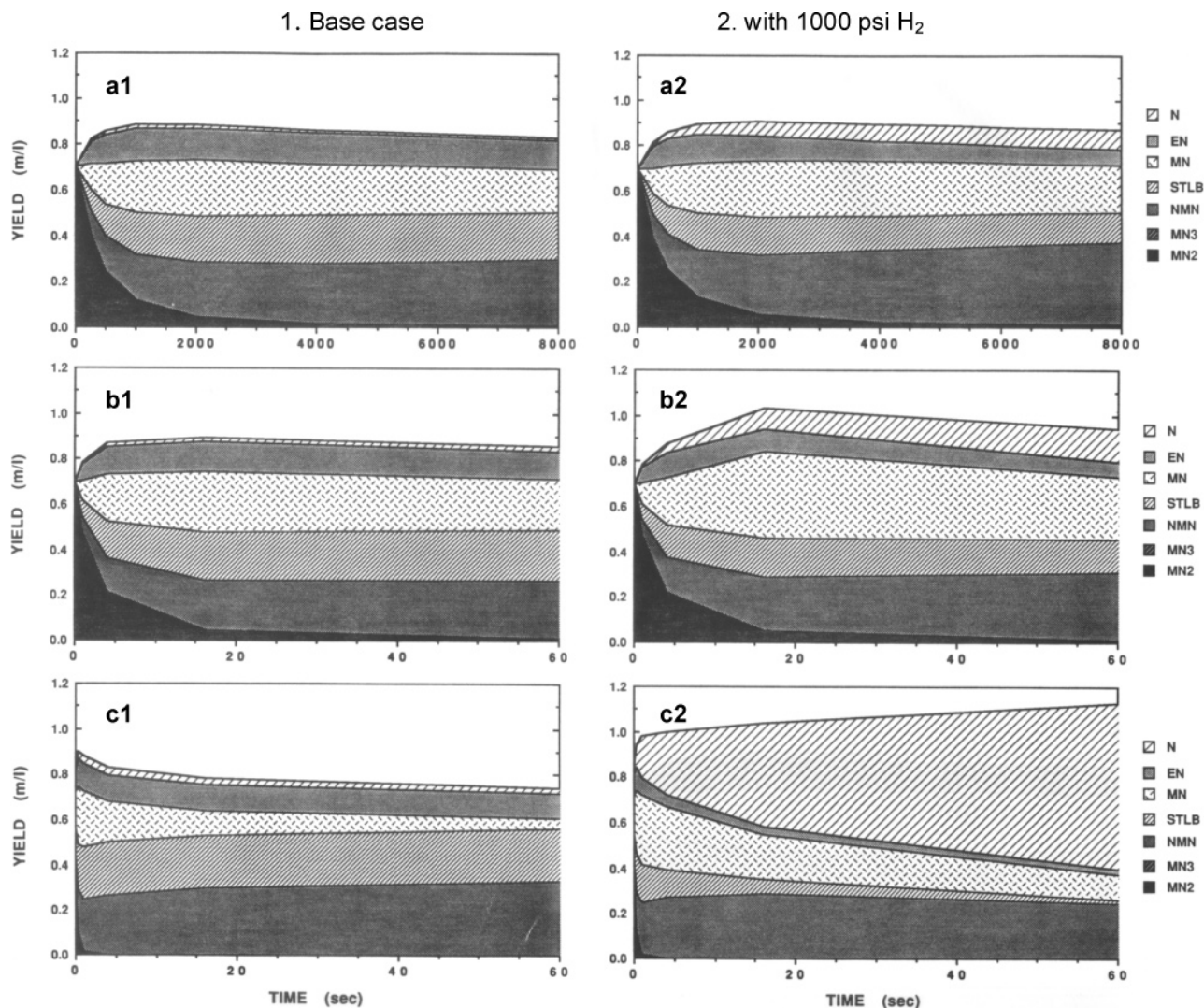
Retrograde Products in Coal Conversion

J. Phys. Chem. A, Vol. 110, No. 21, 2006 **6767**

Figure 2. Computed impact of added hydrogen on the evolution of cleavage and retrograde products at (a) 400 °C, (b) 500 °C, and (c) 600 °C. (Note that the thin sliver of MN3 is not visible in these figures.)

TABLE 6: Relative Yields of Cleaved and Uncleaved Products as a Function of Temperature and H$_2$ Pressure

temp (°C)	time (s)	Σ (MN, EN, N) (cleaved products)		% uncleaved products (MN2, MN3, NMN, STLB)	
		H$_2$ = 0	H$_2$ = 1000 psi	H$_2$ = 0	H$_2$ = 1000 psi
400	8000	0.33	0.38	61	58
500	60	0.38	0.51	58	48
600	60	0.18	0.81	75	23
	2	0.40	0.74	53	41

TABLE 7: Computed Relative Effectiveness of Hydroaromatic Donor and 1000 psi H$_2$ as Scavengers[a]

temp (°C)	time (s)	[H$_2$]/ [PhenH$_2$]	scav by H$_2$/ scav by PhenH$_2$	% recombination of benzylic fragments	
				H$_2$ = 0	H$_2$ = 1000 psi
400	250	44	0.15	11	11
500	1	33	0.39	41.5	41
600	0.06	37	1.1	91	89

[a] Computed using the reaction system shown in Scheme 3 and Table 4. Starting concentrations: [MN2] = 0.7 M, [PhenH$_2$] = 0.1 M, [Phen] = 0.5 M, [H$_2$] as indicated.

500 °C and 8000 s at 400 °C computations. The very marked increase in the impact of H$_2$ at 600 °C is in accord with the experimental observation[42] that the effect of H$_2$ pressure in rapid-heating coal pyrolyses is generally not significant until the temperature exceeds 600 °C, where equilibrium between H$_2$ and H$^\bullet$ is approached.

Given the very pronounced effect of H$_2$ on hydrogenolysis to produce N, it is even more striking that it has rather little impact on the yield of the true retrograde product NMN, even at 600 °C. While it increases the yields of MN and N by factors of 4 and 20, and decreases the stilbene analogue to almost nothing, the presence of H$_2$ decreases the NMN yield by only about 30%, as shown in Figure 2. Clearly, the reactions included in this model do show H$_2$ to increase bond cleavage significantly at all temperatures but do not show it substantially preventing the generation of those retrograde products that are formed
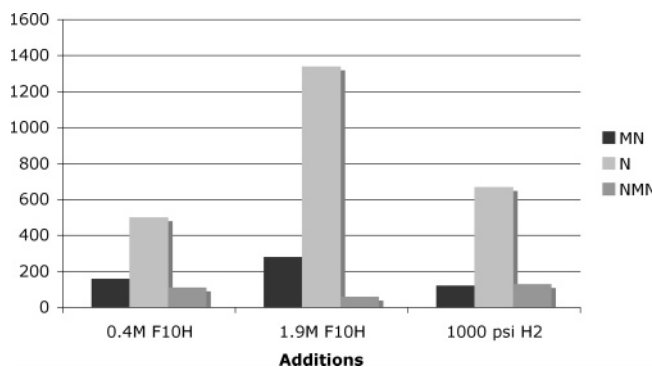
through the addition of resonance-stabilized radicals. Examination of individual reaction rates reveals that, at 600 °C, 1000 psi H$_2$ decreases the initial net rate of NMN production only by 2%, relative to its value in the absence of H$_2$. At 500 °C, initial NMN production is actually increased slightly, and at 400 °C and 1000 s (~80% consumption of the starting structure MN2), the net rate of NMN production increased by 25%! Only at 600 °C and at long reaction times is there ever a substantial net consumption of NMN in hydrogenolysis reactions as a result of added H$_2$ pressure.

According to the model, the presence of H$_2$, in its action as a scavenger, can sometimes serve to increase the rate of retrograde product formation. The rate of strong bond scission

TABLE 8: Computed Impact of H$_2$ Pressure at 600 °C on Maintaining Hydroaromatic Level and on Naphthalene-Producing Hydrogenolysis[a]

	[PhenH$_2$] (m/l)		% increase	relative d[naphthalene]/dt (M^{-1} s^{-1})		% increase
time (s)	H$_2$ = 0	1000 psi H$_2$	in [PhenH$_2$]	H$_2$ = 0	1000 psi H$_2$	in d[N]/dt
0.016	0.0903	0.0907	0.4	1.0	2.27	127
0.063	0.0707	0.0736	4	0.51	1.84	261
0.25	0.040	0.048	22	0.12	0.80	560
1.0	0.015	0.026	85	0.01	0.23	2200
4.0	0.003	0.015	400	−0.001	0.08	

[a] Computed using the reaction system shown in Scheme 3 and Table 4. Starting concentrations: [MN2] = 0.7 M, [PhenH$_2$] = 0.1 M, [Phen] = 0.5 M, [H$_2$] as indicated.

Figure 3. Computed impact of added hydroaromatic and hydrogen pressure on scavenging, hydrogenolysis, and retrograde products.

induced by H-transfer is also increased, such that, over the entire reaction time, the net rate of NMN formation is decreased. Thus, the presence of H$_2$ does not inhibit NMN formation per se; the net reduction in NMN is a result of faster hydrogenolysis.

Table 7 shows the computed relative effectiveness of a low level of indigenous hydroaromatic (0.1 M starting concentration of 9,10-dihydroaromatic) and of added H$_2$ pressure in capping the fragment radicals and preventing their recombination. At 400 °C, scavenging by H$_2$ is only 15% of that by the hydroaromatic, despite the fact there is a 40-fold molar excess of H$_2$. At higher temperatures, the excess of H$_2$ declines as it becomes an increasingly important scavenger. Higher temperatures make the highly endothermic scavenging by H$_2$ increasingly important, and it is substantially consumed as the reaction progresses, thereby maintaining the hydroaromatic content closer to its original level. However, at all temperatures, 1000 psi H$_2$ decreases the fractional recombination of the fragment radicals by no more than a few percent.

The results in Table 7 illustrate what we can anticipate from the thermochemistry of hydrogen transfer, namely, that even at the minimal starting concentration of hydroaromatic (0.1 M), scavenging by 1000 psi H$_2$ (even with no transport limitations) appears less important than scavenging by the hydroaromatic. This finding further suggests that the major impact of H$_2$ does not really lie in its acting as a successful scavenger (as had often been claimed in the literature) but rather lies in some other factor. To explore this issue, additional runs were performed for comparison with the base case (which had 0.1 M dihydrophenanthrene and no added H$_2$). Figure 3 compares the impact of adding 0.4 or 1.9 M hydroaromatic with that of 1000 psi H$_2$ at 500 °C. As anticipated from Table 7, even the smaller amount of added hydroaromatic resulted in a greater increase in scavenged product (methylnaphthalene) than did 1000 psi H$_2$. The added hydrogen is slightly poorer at increasing scavenging (to give MN) and poorer at inhibiting the retrograde product (NMN) yield but slightly better at increasing the hydrogenolysis product (naphthalene). Addition of 1.9 M dihydrophenanthrene is shown to be superior in all respects to 1000 psi H$_2$.

The modeling study also makes it clear that the impact of added H$_2$ on hydrogenolysis, at least in the short run, does *not* come primarily through its maintenance of a useful hydroaromatic content, as has often been postulated in the liquefaction context. Hydrogen pressure most assuredly does help to maintain the hydroaromatic level, and hydrogenolysis activity is certainly generated by these hydroaromatics, but higher hydroaromatic content is a result, rather than a cause, of the hydrogenolysis activity resulting from the presence of H$_2$. This causal relationship was established through examination of the output of the model at very short reaction times, where the presence of added H$_2$ has not yet had the opportunity to make a significant impact on the dihydrophenanthrene content but changes in the various steady-state radical populations have been established. Table 8 shows computed values for dihydrophenanthrene concentration and for the net rate of naphthalene production by various hydrogenolysis reactions.

The values in Table 8 that show the impact of added H$_2$ on dihydrophenanthrene content at short reaction times to be marginal (+0.4% at 0.016 s), but the total impact on the modeled hydrogenolyses that produce naphthalene to be very substantial (127%), are a good indicator that the main impact on hydrogenolysis is a direct rather than indirect result of H$_2$. At progressively longer reaction times, the percentage increase in hydroaromatic becomes relatively more important, but for all reaction times in Table 8, it is always less than the instantaneous increase in the rate of naphthalene formation. Though quantitatively surprising, the overall result is consistent with the experimental results of Vernon, who found that, above ~450 °C and ~500 psi H$_2$, added H$_2$ in the presence of homolytically generated benzylic radicals resulted in measurable hydrogenolysis of strong bonds.[10] Our results indicate further that the highly endothermic scavenging by H$_2$ has its most pronounced effect directly through the H-atoms produced in the scavenging, rather than indirectly through increased donor content that also results. In fact, the sum of scavenging due to H$_2$ and the increased donor content is generally not sufficient to decrease the initial rate of formation of the true retrograde product, NMN. As Figure 2 shows, the computed rates of NMN formation actually increase at 400 and 500 °C.

Summary and Conclusions

The formation of retrograde products via the addition of resonance-stabilized radicals appears typically not to be a facile reaction in homogeneous model systems involving two- to four-ring aromatic systems. Thermochemical estimates and numerical modeling indicate that special factors will typically be necessary for such retrograde reactions to be important. Examples of these special factors were seen to include the following: (1) aromatic clusters particularly susceptible to radical addition, (2) the presence of readily displaceable radical fragments, and/or (3) the presence of aromatic systems or steady-state radical

Retrograde Products in Coal Conversion

J. Phys. Chem. A, Vol. 110, No. 21, 2006 **6769**

concentrations that are capable of rapid bimolecular reaction with the unstable retrograde adducts to accept a hydrogen and stabilize the adduct. A mechanistic model was used to explore the factors affecting the formation of stable retrograde products via the addition of aralkyl radicals, using conditions designed to make such product formation particularly favorable. These were (1) a coal surrogate designed to produce high concentrations of such radicals through the homolysis of weak ethylene linkages between naphthalene rings and (2) naphthalene thermochemistry modified to make addition 4 kcal/mol more favorable than the accepted heats of formation values would dictate.

The computed results illustrate that if the concentration of attacking radicals is higher than can be generated by the scavenger system working in its *initiator* capacity, then the better scavenger *may* more effectively prevent retrograde product formation. This will be the case if the better scavenging capability decreases the attacking radical concentration more than its H-atom accepting capability increases the fraction of the initial adducts that are successfully stabilized. At short reaction times, the yield of retrograde products from a "burst" of homolytically generated benzylic radicals was lower when dihydroanthracene (rather than dihydrophenanthrene) was the hydroaromatic scavenger. However, at long reaction times, when the main source of benzylic attacking radicals is the radical soup itself, the higher radical concentration provided by the better scavenger acted to generate more attacking radicals and also to more readily stabilize the adducts.

Numerical modeling shows that dihydroanthracene, through its better scavenging, tends to decrease the yield of the recombination product MN3 at short reaction times but *increase* the yield of the true retrograde product NMN at long reaction times. This result is in accord with the long-recognized but somewhat paradoxical result that 9,10-dihydroanthracene, by far the best scavenger among hydroaromatics in two-, three-, and four-ring systems, is by a significant margin *not* the best coal liquefaction solvent.

Finally, the modeling results indicate that the beneficial effects of H$_2$ pressure in short-reaction-time, thermal coal gasification and liquefaction, in contrast to what has often been asserted in the literature, are *not* primarily due to the lowering of harmful radical concentrations by scavenging, *nor* to the maintenance of donor content. The "scavenging" by H$_2$ that does take place is beneficial primarily because the small population of free H-atoms produced is very active in causing increased scission of strong bonds. In fact, the computations show that strongly bonded retrograde products under some conditions are actually generated *faster* with added H$_2$, but at longer reaction times and higher temperatures, this temporary disadvantage of H$_2$ is overcome by increased hydrogenolysis of those earlier-produced retrograde products.

Thus, with donor solvents as well as with H$_2$ pressures, the computed impact on one general class of retrograde products is seen, in respect to the effects discussed, to be completely in accord with experimental results but often in contrast with the accepted mechanistic rationalizations. Somewhat ironically, these results also indicate that the very important aspect of retrograde reactions in coal liquefaction, pyrolysis, and gasification is difficult to counteract directly and that many ameliorative approaches do not so much block retrogression itself as they act by hydrogenolysis of retrograde products once formed. In other words, not only the cleavage of critical bonds in the original coal structures but also the *net* prevention of retrogres-

sion may be due to the H-transfer-induced cleavage of strong bonds.

References and Notes

(1) Deffeyes, K. S. *Beyond Oil: The View from Hubbert's Peak*; Hill and Wang: New York, 2005; pp 35−51.
(2) Campbell, C. J.; Laherrere, J. H. *Sci. Am.* **1998**, 78.
(3) Maugeri, L. *Science* **2004**, *304*, 1114.
(4) McMillen, D. F.; Malhotra, R.; Hum, G. P.; Chang, S.-J. *Energy Fuels* **1987**, *1*, 193.
(5) Stein, S. E. Free Radicals in Coal Conversion. In *Chemistry of Coal Conversion*; Schlosberg, R. H., Ed.; Plenum Press: New York, 1985; p 13.
(6) Buchanan, A. C.; Dunstan, T. D. J.; Douglas, E. C.; Poutsma, M. L. *J. Am. Chem. Soc.* **1986**, *108*, 7703.
(7) McMillen, D. F.; Malhotra, R.; Chang, S.-J.; Fleming, R. H.; Ogier, W. C.; Nigenda, S. E. *Fuel* **1987**, *66*, 1611.
(8) McMillen, D. F.; Malhotra, R.; Nigenda, S. E. *Fuel* **1989**, *68*, 380.
(9) Malhotra, R.; McMillen, D. F.; Tse, D. S.; St. John, G. A. *Energy Fuels* **1989**, *3*, 465.
(10) Vernon, L. W. *Fuel* **1980**, *59*, 102.
(11) Ross, D. S.; Blessing, J. E. Possible Hydride Transfer in Coal Conversion Processes. In *Coal Liquefaction Fundamentals*; Whitehurst, D. D., Ed.; ACS Symposium Series 139; American Chemical Society: Washington, DC, 1980; p 301.
(12) McMillen, D. F.; Malhotra, R.; Chang, S.-J.; Nigenda, S. E.; St. John, G. A.; *Fuel* **2004**, *83*, 1455.
(13) McMillen, D. F.; Ogier, W. C.; Ross, D. S. *J. Org. Chem.* **1981**, *46*, 3322.
(14) Malhotra, R.; McMillen, D. F. *Energy Fuels* **1990**, *4*, 184.
(15) Ettinger, M. D.; Mahasay, S. R.; Stock, L. M.; Zabransky, R. F. *Energy Fuels* **1987**, *1*, 274.
(16) Zabransky, R. F.; Stock, L. M. *Thermally Initiated Carbon−Carbon Bond Cleavage Reactions Occurring During Coal Gasification, Final Report*; GRI-88/0272; Gas Research Institute: Chicago, IL, 1988.
(17) Ofosu-Asante, K.; Stock, L. M.; Zabransky, R. F. *Fuel* **1989**, *68*, 567.
(18) Since there is not a universal understanding of the words "homolysis" and "thermolysis", we will define these terms for the purpose of this paper in agreement with their most common usage. "Homolysis" will be taken to mean thermally induced, unimolecular homolytic scission of a bond to produce two free radicals. "Thermolysis", on the other hand, will be used to refer to the assemblage of reactions that result from heating a chemical substance or mixture of substances. For compounds that are predominantly H−C−O structures, these reactions, in the absence of heterogeneous catalysts, will tend to be largely those involving the formation or destruction of uncharged free radicals.
(19) Squire, K. R.; Solomon, P. R.; Carangelo, R. M.; DiTaranto, M. B. *Fuel* **1986**, *65*, 833.
(20) Solomon, P. R.; Hamblen, D. G.; Carangelo, R. M.; Serio, M. A.; Deshpande, G. V. *Combust. Flame* **1988**, *71*, 137.
(21) Squire, K. R.; Solomon, P. R.; DiTaranto, M. B. *Synthesis and Study of Polymer Models Representative of Coal Structure - Phase II, Final Report, GRI-81/0171*; Gas Research Institute: Chicago, IL, 1985.
(22) Benson, S. W. *Thermochemical Kinetics*, 2nd ed.; John Wiley and Sons: New York, 1976.
(23) McMillen, D. F.; Golden, D. M. *Annu. Rev. Phys. Chem.* **1982**, *33*, 493.
(24) Stein, S. E. A Fundamental Chemical Kinetics Approach to Coal Conversion. In *New Approaches in Coal Chemistry*; Blaustein, B. D., Bockrath, B C., Friedman, S., Eds.; ACS Symposium Series 169; American Chemical Society: Washington, DC, 1981; p 97.
(25) Herndon, W. C. *J. Org. Chem.* **1981**, *46*, 2119.
(26) Miller, R. E.; Stein, S. E. *J. Phys. Chem.* **1981**, *85*, 580.
(27) Benson, S. W.; O'Neal, H. E. *Kinetic Data on Gas-Phase Unimolecular Reactions*; National Standard References Data Series NSRDS-NBS 21; National Bureau of Standards: Washington, DC, 1970.
(28) Cox, J. D.; Pilcher, G. *Thermochemistry of Organic and Organometallic Compounds*; Academic Press: New York, 1970.

(29) Pedley, J. B.; Naylor, R. D.; Kirby, S. P. *Thermodynamics of Organic Compounds*; Chapman and Hall: New York, 1986.

(30) Tsang, W. *J. Am. Chem. Soc.* **1985**, *107*, 2872.

(31) Tsang, W. *J. Phys. Chem.* **1986**, *90*, 1152.

(32) Manka, M.; Stein, S. E.; *J. Phys. Chem.* **1984**, *88*, 5914.

(33) Lehni, M.; Schuh, H.; Fischer, H. *Int. J. Chem. Kinet.* **1979**, *11*, 705.

(34) Senthilnathan, V. P.; Stein, S. E. *J. Org. Chem.* **1988**, *53*, 3000.

(35) Stein, S. E.; Griffith, L. L.; Billmers, R.; Chen, R. H. *J. Org. Chem.* **1987**, *52*, 1582.

(36) Fahr, A.; Stein, S. E. *J. Phys. Chem.* **1988**, *92*, 4951.

(37) Chen, R. H.; Kafafi, S. A.; Stein, S. E. *J. Am. Chem. Soc.* **1989**, *111*, 1418.

(38) Stein, S. E.; Robaugh, D. A.; Alfieri, A. D.; Miller, R. E. *J. Am Chem. Soc.* **1982**, *104*, 6567.

(39) Buchanan, A. C.; Dunstan, T. D. J.; Douglas, E. C.; Poutsma, M. L. *J. Am. Chem. Soc.* **1986**, *108*, 7703.

(40) Billmers, R.; Griffith, L. L.; Stein, S. E. *J. Phys. Chem.* **1986**, *90*, 517.

(41) Bockrath, B. C.; Bittner, E.; McGrew, J. *J. Am. Chem. Soc.* **1984**, *106*, 135.

(42) Howard, J. B. Fundamentals of Coal Pyrolysis and Hydropyrolysis. In *Chemistry of Coal Utilization* (Second Suppl. Vol.); Elliot, M. A., Ed.; Wiley-Interscience: New York, 1981; Chapter 12.

(43) Gavalas, G. R. *Coal Pyrolysis*; Elsevier: Amsterdam, The Netherlands, 1982.